Ioffe Institute
6th Int. Symp. "Nanostructures: Physics and Technology"
St Petersburg, Russia, June 22–26, 1998.

Fabrication of metallic nanostructures by local oxidation with a scanning probe microscope

R. J. M. Vullers, M. Ahlskog and *C. Van Haesendonck*
Laboratorium voor Vaste-Stoffysica en Magnetisme, Katholieke Universiteit Leuven
Celestijnenlaan 200 D, B-3001 Leuven (Belgium)

Abstract. Surfaces can be oxidized with the tip of a scanning probe microscope when applying a voltage between surface and tip. The oxidation process is voltage and humidity dependent, and can be explained in terms of anodic oxidation. The local oxidation allows the nanoscale patterning of doped silicon wafers as well as of metal films. In the case of silicon, the thin oxide layer can serve as an effective mask in a wet etching step. Sufficiently thin metal films (e.g., Ti or Al) can be completely oxidized down to the substrate, enabling the direct writing of nanostructures.

1 Introduction

The scanning probe microscope (SPM) has emerged as a powerful tool for modifying various surfaces at the nanometer scale [1]. While atomic manipulation is the ultimate goal, such a manipulation technique does not allow to fabricate stable structures under ambient conditions. On the other hand, the SPM offers a valuable alternative to the classical high-energy electron beam lithography. The low-energy beam, which is produced by the tip of a scanning tunneling microscope (STM), allows to locally expose thin resist layers and obtain linewidths as small as 20 nm.

The local oxidation of surfaces with an SPM was demonstrated for the first time by Dagata et al. [2]. These authors were able to transform a passivated silicon surface into a thin silicon oxide layer when applying a sufficiently large voltage between the tip of an STM and the Si surface. It was shown that the oxidation of the Si can also be achieved with the metallized tip of an atomic force microscope (AFM) [3]. The written oxide lines, which can be as narrow as 10 nm [4], can afterwards be inspected with the AFM, without inducing any further oxidation. The local oxidation of Si surfaces has been used to prepare a submicrometer side-gated MOSFET transistor [5]. SPM induced oxidation is also possible for various metal films which, when sufficiently thin, can be completely transformed into an oxide down to the substrate [6]. The local oxidation of Ti films has enabled the fabrication of a single electron transistor (SET) with lateral tunneling barriers [7]. Single-atom point contacts could be obtained by locally oxidizing an Al strip [8].

2 The local oxidation technique

2.1 Theoretical background

Since the local oxidation is performed under ambient conditions, a water layer is always present on the sample surface. When the sample is biased positively with respect to the tip, the surface starts to be oxidized when exceeding a treshold voltage. The oxidation process can be described in terms of anodic oxidation, with the water acting as an

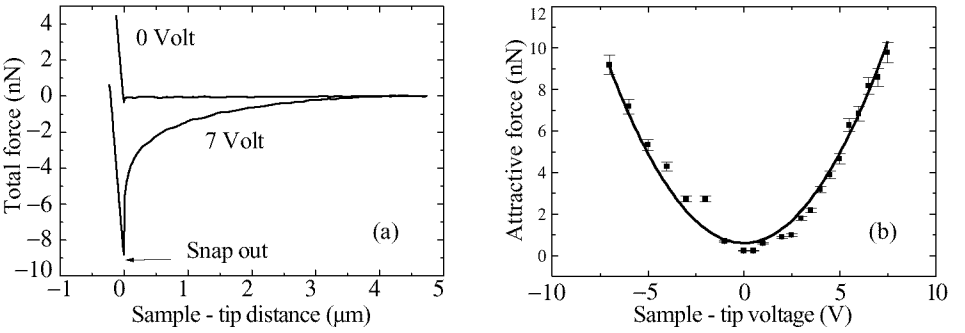

Fig 1. (a) Force versus distance curves for zero applied voltage and for $V = 7\,\mathrm{V}$. (b) The attractive force between tip and sample for different applied voltages.

electrolyte. Conventional electrochemical anodization requires a treshold electrical field $\sim 10^7\,\mathrm{V/cm}$ for anodization [9]. Ionic diffusion of OH^- or O^- occurs through the oxide layer (the exact nature of the diffusing specie is not known) towards the interface with the non-oxidized part of the sample [10]. Since a condensed water layer acts as the electrolyte, the amount of water on the surface and hence also the humidity play an essential role. It has been found for both Si [11] and Ti [12], that an increase in humidity increases the size of the written oxide lines. Stiévenard et al. [13] have suggested that the local oxidation is consistent with the Cabrera-Mott theory [14] of electrical field enhanced oxidation. Other experiments do, however, find deviations from the Cabrera-Mott model for the oxide growth [15].

2.2 *Influence of the tip geometry*

The actual shape of the tip is important, since it determines the electrical field distribution. On the other hand, prolonged use of the same tip results in a degradation of the tip shape due to wear. For an AFM the wear is a result of the attractive electrostatic force which appears between the tip and sample when applying a voltage. The force F_{el} depends on the tip-sample distance z, the tip-sample capacitance C, and the applied voltage V:

$$F_{el} = \frac{dC}{dz} V^2 \quad . \tag{1}$$

The presence of a water layer will cause an additional attractive capillary force F_{cap}, resulting in a total attractive force

$$F_{att} = F_{cap} + \frac{dC}{dz} V^2 \quad . \tag{2}$$

When operating an AFM in the contact mode, the attractive forces will not cause an extra deflection of the cantilever. The only possible way to measure the extra forces is an analysis of the force-distance curves: Starting in contact, the tip is retracted and at the same time the cantilever deflection is measured. At first, the repulsive force will decrease, decreasing the bending of the cantilever. Due to the attractive force, the tip will remain in contact, even when the repulsive force has become zero. The cantilever will start to bend the other way, pulling at the tip. As soon as the pulling force equals

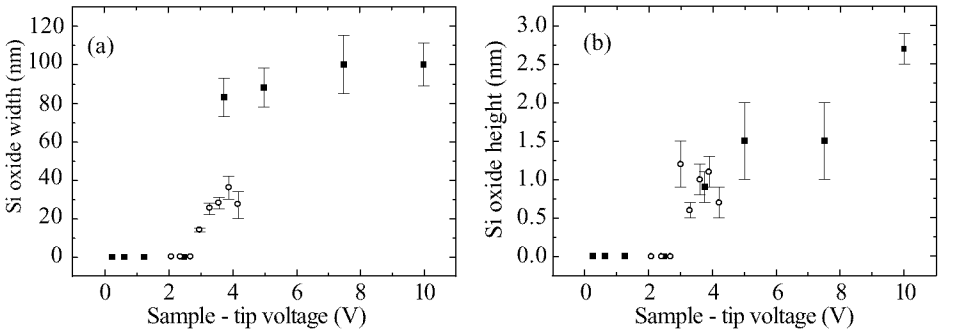

Fig 2. Width (a) and thickness (b) of Si oxide lines which have been written with an AFM at different applied voltages. The open and closed symbols refer to the results obtained with two different AFM tips.

the attractive forces, the tip will suddenly loose contact (snap out). Increasing the applied voltage, increases the attractive force. A typical result, which has been obtained in Leuven for a Ti film, is shown in Fig. 1(a). The attractive force is obtained from the difference between the snap out force and the force acting at long distances, i.e., $F = 0$. At zero voltage, the small deflection is entirely due to F_{cap}. Plotting the attractive force against the applied voltage, clearly reveals a V^2 dependence, as illustrated in Fig 1(b).

3 Patterning of silicon wafers

3.1 The local oxidation process

For our experiments, we have used n-type, (100) oriented Si wafers with a resistivity of 10 mΩcm. Before starting the oxidation process, the silicon surface has to be cleaned and the native oxide needs to be removed. This can be done by immersing the sample in a bath of hydrofluoric acid (HF). The native oxide layer is etched away and replaced by a mono-atomic passivation layer which consists of H atoms attached to a clean Si surface layer. Next, a positive voltage is applied under ambient conditions between the Si and a Ti coated AFM tip. We have written lines with different voltages. After reducing the voltage back to zero, the written oxide lines are imaged with the same AFM tip. As shown in Fig. 2, there exists a threshold voltage (about 3 V) below which no oxide is formed. The oxide thickness is approximately 3 nm for an applied voltage of 10 V. The local oxidation can also be performed with an STM. We have written oxide lines for different values of the tunneling current which is maintained constant during the scanning process. No current dependence could be observed, consistent with an anodic oxidation process.

3.2 The etching process

Due to the different etching speed of the silicon oxide when compared to the silicon, the written oxide patterns can be used as an effective mask in a wet etching process. Using TMAH (tetra-methyl ammonium hydroxide), a selectivity of 1000 can be achieved [16], allowing to easily transfer the written pattern into the silicon wafer. There also exists a difference in etching speed between the (100) and (111) directions, causing the lines to be etched under an angle of 55° for a (100) oriented surface. In order to write more complicated structures, one needs to be able to move the tip along a predefined

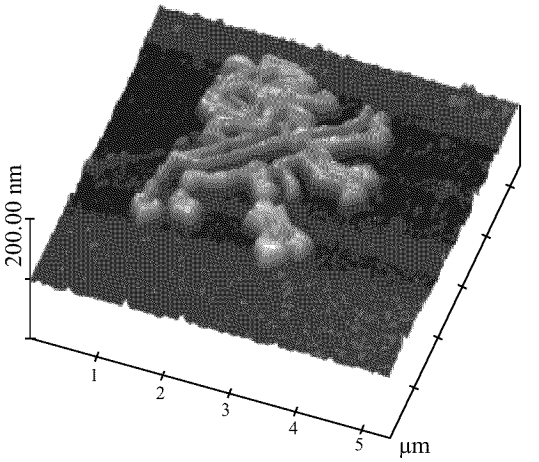

Fig 3. AFM picture of a mesoscopic lion obtained by local oxidation with an STM and subsequent etching of a Si wafer.

pattern (vector scan). We have made the necessary adaptions of the electronics and the software of our SPM system (Park CP) to obtain an improved control of the tip motion. The structure shown in Fig. 3 has been written with the STM and imaged with the AFM after etching.

4 Local oxidation of Ti films

While the silicon oxidation technique usually involves two or more steps for the fabrication of conducting mesoscopic structures, the oxidation of Ti can be used as a direct, single step patterning process. When using a thin Ti film, one can fabricate the desired pattern by oxidizing completely through the film, thus separating the conducting regions by an oxide.

4.1 The oxidation process

Ti films having a thickness between 5 and 10 nm have been deposited onto oxidized Si substrates by dc magnetron sputtering. The local oxidation of these films is performed with an AFM with diamond coated tips (resistivity 2.5 mΩcm, thickness 100 nm). TiO_x lines are written at different scanning speeds and for different voltages applied between the Ti film and the tip. Figure 4(a) shows the variation of the height of the oxide line when moving the AFM at different speeds. The height changes linearly with the logarithm of the writing speed [15]. Figure 4(b) shows the dependence of the height of the lines on the applied bias voltage. The treshold voltage above which we start to write oxide lines turns out to be in the vicinity of 5 V for the diamond coated tips.

4.2 Fabrication of narrow Ti lines

In the inset of Fig. 5(a) we show a schematic view of our process for fabricating very narrow Ti lines. Combining electron beam lithography and lift-off techniques, we first prepare a wider Ti line (width $w_0 = 2\,\mu$m). Next, the width of the line is gradually reduced by oxidizing the outer parts of the line with the tip of our AFM. During the oxidation process the tip is scanned back and forth along horizontal lines (see arrows in

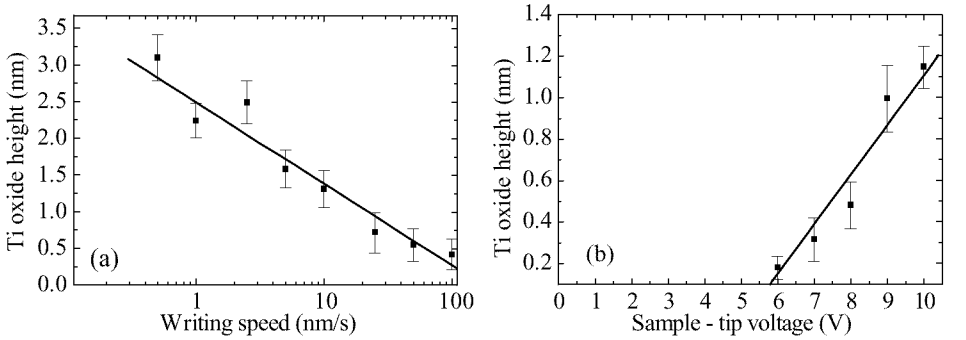

Fig 4. (a) Height of the written TiO_x lines for different writing speeds. (b) Height of the oxide lines for different applied voltages.

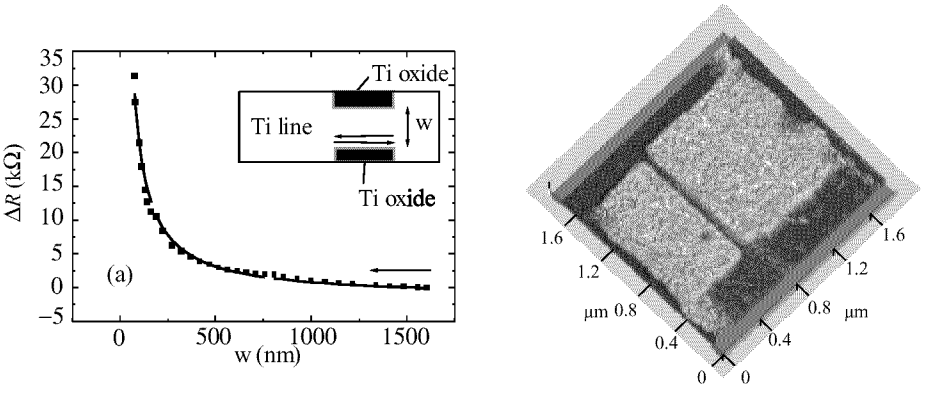

Fig 5. (a) The resistance change ΔR of a Ti line when reducing its width w with the local oxidation technique (see inset). (b) AFM picture of the Ti line after the oxidation process.

the inset of Fig. 5(a)), reducing the metallic Ti gap to a width w. During the oxidation process the resistance of the remaining metallic Ti line is continuously monitored. The change in resistance ΔR is plotted against the width of the remaining gap in Fig. 5(a). Starting from the larger widths w, the resistance continuously increases with decreasing width. The data can be fitted using the simple relation

$$\Delta R = \rho \frac{L}{d} \left(\frac{1}{w} - \frac{1}{w_0} \right) , \tag{3}$$

with ρ the resistivity of the Ti film, L the length of the constriction and d the thickness of the Ti film.

When the resistance reaches 30 kΩ, the oxidation is stopped by turning off the voltage and the fabricated Ti line can be imaged with the AFM. The topographical image is shown in Fig. 5(b). The brighter areas correspond to the oxide, while the darker areas correspond to the non-oxidized parts of the Ti film. The width of the remaining Ti line is 74 nm.

This work has been supported by the Fund for Scientific Research - Flanders (FWO)

as well as by the Flemish Concerted Action (GOA) and the Belgian Inter-University Attraction Poles (IUAP) research programmes.

References

[1] For a review, see E. S. Snow et al., *Proceedings of the IEEE* **85** 601 (1997).
[2] J. A. Dagata et al., *Appl. Phys. Lett.* **56** 2001 (1990)
[3] H. C. Day and D. R. Allee, *Appl. Phys Lett.* **62** 2691 (1993).
[4] E. S. Snow et al., *Appl. Phys. Lett.* **66** 1729 (1995).
[5] P. M. Campbell et al., *Appl. Phys. Lett.* **66** 1388 (1995).
[6] For a review, see K. Matsumoto, *Proceedings of the IEEE* **85** 612 (1997).
[7] K. Matsumoto et al., *Jpn. J. Appl. Phys.* **34** 1387 (1995).
[8] E. S. Snow et al., *Appl. Phys. Lett.* **69** 269 (1996).
[9] S. K. Ghandi, *VLSI Fabrication Principles* (Wiley, New York, 1983)
[10] A. E. Gordon et al., *J. Vac. Sci. Technol. B* **13** 2805 (1995).
[11] H. Sugimura et al., *Appl. Phys. Lett.* **65** 1569 (1994).
[12] H. Sugimura et al., *Appl. Phys. Lett.* **63** 1288 (1993).
[13] D. Stiévenard et al., *Appl. Phys. Lett.* **70** 3272 (1997).
[14] N. Cabrera and N. F. Mott, *Rep. Prog. Phys.* **12** 163 (1948).
[15] Ph. Avouris et al., *Appl. Phys. Lett.* **71** 285 (1997).
[16] O. Tabata et al., *Sensors and Actuators* **34** 51 (1992).